Zhang *et al. Stem Cell Research & Therapy* (2025) 16:562
https://doi.org/10.1186/s13287-025-04677-9

Stem Cell Research & Therapy

RESEARCH Open Access

BMDMs in metabolic memory impair fracture healing in diabetes

Dong Zhang[1*], Changjiang Liu[1], Ying Yuan[1], Junwei Su[1], Zheng Wang[1], Chao Jian[1*] and Aixi Yu[1*]

Abstract

Background The risk of fractures nonunion and delayed union in diabetes mellitus remains elevated despite glucose-lowering therapies. We hypothesized that bone marrow-derived macrophages (BMDMs) can be induced in the status of metabolic memory and still impair fracture healing when hyperglycemia stimulus disappears.

Methods Diabetic mice were divided into control (Ctrl), diabetic (DM), and diabetic with glucose control (DM/GC) groups. Fracture healing was assessed by micro-CT and histology, evaluating callus volume, bone volume/total volume (BV/TV), and inflammatory markers. In vitro, bone marrow-derived macrophages (BMDMs) were exposed to high glucose (HG) for varying periods to simulate hyperglycemia-induced metabolic memory, followed by normalization. Pro-inflammatory cytokines and macrophage polarization (M1/M2) were assessed via ELISA and flow cytometry. Osteogenesis and angiogenesis were evaluated in co-culture assays. RNA-seq and ATAC-seq were performed to analyze gene expression and chromatin accessibility, focusing on inflammatory pathways and CEBPB.

Results All data show that BMDMs play a significant role in the sustained effects of hyperglycemia on fracture healing even after glucose normalization in diabetic animals. Hyperglycemia-induced metabolic memory in BMDMs resulted in increased pro-inflammatory cytokines and a higher proportion of M1 macrophages, which impaired osteogenesis and angiogenesis. The co-culture medium from BMDMs in metabolic memory conditions suppressed osteogenesis in BMSCs and angiogenesis in HUVECs. Integrated analysis of RNA-seq and ATAC-seq in BMDMs revealed that inflammatory pathways were upregulated, with CEBPB identified as a key factor. Silencing CEBPB reversed these adverse effects and enhanced fracture healing in a diabetic model.

Conclusions Our results demonstrate the reason why the glucose-lowering therapies is unsuccessful in reducing the risk of fractures nonunion and delayed union in patients with diabetes mellitus, and shed light on a new strategy for the disease.

Keywords Metabolic memory, BMDM, Diabetes, Bone healing, CEBPB

*Correspondence:
Dong Zhang
zhangdongemail@whu.edu.cn
Chao Jian
chaojian@whu.edu.cn
Aixi Yu
yuaixi@whu.edu.cn
[1]Department of Orthopedics Trauma and Microsurgery, Zhongnan Hospital of Wuhan University, Wuhan 430071, China

Introduction

Currently, more than 537 million people suffer from diabetes mellitus (DM), and the prevalence of the disease leads to life-threatening, disabling, and costly complications, and seriously impairs life expectancy and quality worldwide [1]. The major long-term complications of diabetes severely affect the eyes, heart, kidneys, and nerves [2]. It's known that DM and its complications are characterized via hyperglycemia. People used to believe that good glucose-lowering therapies make a favorable prognosis in DM. Unfortunately, recently, data from clinical and observational studies have shown that DM-related complications were highly prevalent even when glucose control was optimal and/or intensive glycemic control was implemented [3–5]. These results signify the status of a "memory" of the prior hyperglycemia exposure in target cells and tissue, which leads to persistence of its adverse effects long after glucose levels are under control.

In recent years, "metabolic memory", which is used to define the persistence of DM complications even after successful glycemic control, has attracted much attention [6]. The term highlighted the information that prior high glucose has sustained effects that persist even after return to more usual glycemic control in diabetes [7]. Studies have shown that metabolic memory is involved in various DM-related complications, such as atherosclerosis, cardiomyopathies, heart failure, kidney disease, cardiovascular and diabetic foot [8–10]. Over the past decades, extensive data and numerous cases demonstrated that DM adversely affects fracture-healing by disturbing the balance of bone homeostasis, and diabetic individuals are at a greater risk of delayed union and nonunion with a doubling of the time to healing of the fracture [11–13]. Yet, to date, whether metabolic memory exists in and persistently harms fracture healing in diabetes, as well as the underlying molecular mechanisms, are still unclear.

Evidence has shown that chronic low-grade inflammation contributes to diabetes-associated complications, and abnormal immune responses in inflammation cells might be the trigger for abnormal immune responses in diabetes [14]. Moreover, immunometabolism, the interplay between cellular metabolism and immune cell function, has been recognized as a fundamental mechanism underlying the pro-inflammatory state in diabetes [15, 16]. This emerging field provides a critical framework to understand how metabolic changes, such as those induced by hyperglycemia, drive immune cell dysfunction and chronic inflammation. Among these inflammation cells, macrophages are regarded as a significant mediator of inflammation primarily in the progression of diabetes mellitus and its complications [17, 18]. They exist in nearly all tissues and are critical for homeostasis, repair, and regeneration [19]. Among them, bone marrow-derived macrophages (BMDMs) can perform as niche cells to osteoblasts and to endotheliocytes, participate in the cell-cell crosstalk and form the signaling network to influence bone repair and regeneration via secreting various bioactive substances [20]. More importantly, our previous and others' studies have shown that BMDMs are in an adverse pathological status caused via hyperglycemia exposure, and produce inflammatory factors including IL-1, TNF-α, iNOS, and so on, thus impeding osteogenesis and angiogenesis, and increasing the probabilities of an uncontrolled regulation of fracture repair [21]. However, whether the metabolic memory phenomenon of BMDMs exists in and impairs diabetic fracture healing, as well as the mechanism underlying transient hyperglycemia-induced BMDMs dysfunction during fracture healing, remain obscure. Therefore, we aimed to elucidate whether metabolic memory is a significant pathogenic factor during fracture repair and regeneration in diabetes, and its underlying mechanism from the perspective of BMDMs.

Methods

Patient characteristics

This study was approved by the Medical Ethics Committee of Zhongnan Hospital of Wuhan University under protocol number 2,021,007. Patients undergoing fracture operations were recruited from Zhongnan Hospital of Wuhan University in China during the period from July 2021 to August 2024. The enrolled patients were categorized into three groups: non-diabetic, poorly controlled diabetes, and intensively controlled diabetes.

Diabetes mellitus (DM) was verified through a review of patients' medical records, with or without the use of antidiabetic medications, or as serum HbA1C levels of ≥ 6.5% (48 mmol/mol) at the time of enrollment in the study, in accordance with the World Health Organization (WHO) guidelines. Patients with HbA1c levels above 7% were classified as having poorly-controlled diabetes, while those with HbA1c levels of 7% or below were considered to have intensively controlled diabetes [22, 23].

Diabetes induction

The animal experiments were approved via the Committee on the Ethics of Animal Experiments of Wuhan University. Experimental protocols were in compliance with the guidelines of the Institutional Animal Care and Use Committee of Wuhan University. All efforts were made to minimize animal suffering. Mice (female, 8 weeks, 18–25 g) were randomly assigned to three groups: control group, diabetic group (DM), and diabetic group with glucose control (DM/GC). Animals without any treatment served as control group. The protocols of establishing diabetic rats have been described in detail previously [24]. Diabetic rats were induced via streptozotocin (150 mg/kg in citrate buffer with pH 4.5, Sigma, USA). One

week later, mice with more than three random blood glucose levels >16.7 mmol/l were classified as being diabetic. After successful diabetes induction, rats in the DM group received no glycemic control for 23 weeks. Rats in the DM/GC groups were kept under uncontrolled hyperglycemia for 4, 8, or 12 weeks, respectively, followed by glycemic control using insulin (8 units per day, administered in two doses) until the end of the 23-week period.

Fracture establishment

All animals were operated under general anesthesia using 1500 mg/kg ketamine hydrochloride before surgery. After the lower Limb was shaved and disinfected, a 1.5-cm incision was created along the proximal femur. Next, the fascia and muscle were pushed aside to expose the femurs. And a transverse femur shaft fracture was created using an oscillating mini-saw. Then, a sterile 27-gauge needle was inserted for intramedullary fixation. Finally, the incision including the subcutaneous tissue and the skin was closed using a 5 – 0 nylon suture. Micro-CT, histological analysis and Western blot analysis of the fractured femurs were made 3 weeks post-operation. At the end of the experiments, rats were humanely euthanized by intraperitoneal injection of sodium pentobarbital (150 mg/kg body weight), and death was confirmed by the absence of respiration and heartbeat, in accordance with institutional and national ethical guidelines.

Cell culture and transfection

BMDMs were isolated and cultured following previously described methods. Briefly, bone marrow cells were flushed via PBS from the femurs and tibias. To obtain the BMDMs, cells were cultured in RPMI-1640 medium (without glucose) supplemented with 10% fetal bovine serum (FBS) 1% penicillin/streptomycin, and differentiated with 25 ng/ml rat GM-CSF for 7 days, with fresh culture medium supplemented on the 4th day. The glucose concentration in the medium was modified using a glucose solution; to simulate non-diabetic and diabetic conditions in vitro, cells in the normal-glucose (NG) group were cultured in a medium containing 5.5 mM glucose, while the medium for the high-glucose (HG) group was adjusted to 30 mM glucose. To mimic transient hyperglycemia in vitro, BMDMs in the HG/NG group were initially cultured in HG conditions for 5, 10, or 15 days, followed by a return to NG levels until day 20. BMDMs maintained in NG served as a model for physiological glucose levels, while those continuously cultured in HG represented diabetes mellitus (DM) without strict glucose regulation. The hyperglycaemia-induced metabolic memory (MM) group was first incubated in hyperglycemia for 10 days and then returned the normal glucose concentration. After 20 days of culture, BMDMs were followed by treatment with 10 ng/mL IFN-γ plus 100 ng/mL LPS or control media for 16 h and harvested to evaluate the immunomodulation of BMDMs via ELISA, flow cytometry and immunofluorescence.

In vitro Immunomodulation of macrophages

To evaluate macrophage polarization, BMDMs were harvested, washed, and resuspended in PBS containing 1% BSA. Cells were stained with fluorochrome-conjugated antibodies against F4/80, CD86 (M1 marker), and CD206 (M2 marker). The cells were incubated with the antibodies for 30 min at 4 °C, then washed and analyzed by flow cytometry (FACSCanto II, BD Biosciences). The data were analyzed using FlowJo software.

The metabolic profiles of BMDMs were assessed using the Seahorse XFe96 Extracellular Flux Analyzer (Agilent Technologies) according to the manufacturer's instructions. For glycolytic function analysis, extracellular acidification rate (ECAR) was measured following sequential injections of 10 mM glucose, 1 μM oligomycin, and 50 mM 2-deoxyglucose (2-DG). For mitochondrial respiration, oxygen consumption rate (OCR) was assessed after sequential injection of 1.5 μM oligomycin, 2 μM FCCP, and 0.5 μM rotenone/antimycin A. Cytokine levels in the supernatants of BMDMs were measured using commercially available kits, including IL-6, IL-1β, and TNF-α ELISA kits (Elabscience, Wuhan, China). After culturing the BMDMs treated with different concentrations of glucose, the supernatants were collected. ELISA plates were coated with specific capture antibodies, blocked, and incubated with the supernatants. Detection antibodies conjugated to horseradish peroxidase were added, followed by substrate for the enzyme. The optical density (OD) was measured at 450 nm using a microplate reader, and cytokine concentrations were determined by comparing OD values to a standard curve.

To assess the expression of specific markers, cells were fixed in 4% paraformaldehyde for 15 min at room temperature. After washing with phosphate-buffered saline (PBS), permeabilization was carried out using 0.2% Triton X-100 for 10 min. Non-specific binding was blocked with 5% bovine serum albumin (BSA) for 1 h at room temperature. The cells were then incubated with primary antibodies targeting CD86 (1:200) and iNOS (1:200) overnight at 4 °C. Following incubation, the cells were washed and incubated with appropriate fluorescently labeled secondary antibodies for 1 h at room temperature. After counterstaining with DAPI for nuclear visualization, the samples were mounted on slides. The presence of CD86 and iNOS-positive cells was observed under a fluorescence microscope. The results demonstrated a significant increase in CD86 and iNOS expression in BMDMs exposed to HG in different days, suggesting an inflammatory response.

In vitro osteogenic differentiation of BMSCs

BMSCs were isolated and cultured as described previously, and identified by the morphology and flow cytometric analysis. The BMSCs in the passage 3–5 were used in the following experiments. BMSCs were cultured with a mixture of conditioned BMDMs medium and complete medium (1:1), which contained 10 mmol/L β-glycerophosphate disodium salt, 50 μg/ml ascorbic acid, and 10 nmol/L dexamethasone. Alkaline phosphatase (ALP) activity was assessed using the BCIP/NBT staining kit based on the manufacturer's guidelines. On day 14, the fixed cell samples were stained with ARS solution to assess mineralization. The cells were then treated with 10% methylpyridinium chloride for 30 min with gentle shaking. After staining, the BMSCs were washed with PBS and observed using microscopy. Absorbance was then measured at 570 nm–405 nm. Following 14 days of co-culture in different groups, BMSCs were fixed and incubated with 5% goat serum. The cells were then exposed to primary antibodies specific to OPN (22952-1-AP, ProteinTech) and Runx2 (D1L7F, Cell Signaling). After applying fluorescence-conjugated secondary antibodies and counterstaining with DAPI, the samples were examined using confocal laser scanning microscopy (CLSM; TCS SP8, Leica, Germany). The expression levels of Runx2 and OCN were assessed via Western blot. Briefly, total protein was isolated from BMSCs co-cultured for 14 days using RIPA (Aspen) in accordance with the manufacturer's protocol. Proteins were separated by SDS-PAGE, transferred to PVDF membranes, and incubated with primary antibodies against RUNX2, OCN, and β-tubulin. Bands were visualized using ECL and quantified with AlphaEaseFC software.

In vitro angiogenesis of HUVECs

The effect of BMDMs on angiogenesis was determined by Transwell and in vitro scratch wound assays. For the scratch wound assay, when the HUVECs reached 90% confluence, a straight scratch was created. The BMDM media was added to stimulate the HUVEC migration. The HUVECs cells were fixed and then stained with a crystal violet solution for migration observation.

The vessel formation assay for HUVECs involves seeding the cells in a Matrigel matrix (Matrigel, 356231, Corning, USA) to mimic the extracellular environment. The cells are incubated with different conditions, and tube-like structures that form are observed and quantitatively analyzed. This assay assesses angiogenesis by evaluating the network of vessels formed by HUVECs. Besides, the protein expression of VEGF and CD31 was detected by Western blotting.

RNA isolation and RT-qPCR

Total RNA was extracted from BMDMs and tissues using TRIzol reagent, followed by reverse transcription using the HiScript II Q RT SuperMix for qPCR (Vazyme). Quantitative PCR was performed with SYBR Green PCR master mix on a StepOnePlus Real-Time PCR system (Applied Biosystems). The relative gene expression was calculated using the $2^{\wedge -\Delta\Delta}$Ct method, with GAPDH as the reference gene.

ATAC-seq and RNA-seq

For ATAC-seq, Nuclei of BMDMs in MM and NG groups were isolated from the cells, followed by transposition with Tn5 transposase, which integrates sequencing adapters into open chromatin regions. The transposed DNA was then purified and amplified using PCR. The Libraries were validated and sequenced on the Illumina NovaSeq 6000 platform. Data were aligned to the rat genome (Rnor_6.0) using Bowtie2, and chromatin accessibility peaks were called with MACS2. Differential accessibility between conditions was analyzed using DESeq2, followed by Gene Ontology (GO) enrichment analysis using the GREAT tool.

For RNA-seq (RNA Sequencing), total RNA was extracted from BMDMs in MM and NG groups. RNA integrity was checked, and libraries were prepared using the TruSeq Stranded mRNA Library Prep Kit. Poly(A) selection and cDNA synthesis were followed by PCR amplification. Libraries were sequenced on the Illumina NovaSeq 6000 platform. After sequencing, reads were aligned to the rat genome (Rnor_6.0) using STAR. Gene expression was quantified using featureCounts, and differential expression was analyzed with DESeq2, applying a log2 fold change cutoff of >1 and an FDR threshold of 0.05. Gene Ontology and pathway analyses were performed using DAVID or ClusterProfiler, and heatmaps of differentially expressed genes were generated. This approach provided insights into the regulatory mechanisms underlying CEBPB-related changes in macrophage gene expression and chromatin accessibility. Raw RNA-seq and ATAC-seq data supporting the findings of this study are provided in the Supplementary Files.

Western blotting analysis

For protein analysis, cells or tissue samples were lysed in RIPA buffer containing protease and phosphatase inhibitors. Protein concentration was quantified using the BCA protein assay kit. Equal amounts of protein (30 μg) were loaded onto SDS-PAGE gels, transferred to PVDF membranes, and probed with primary antibodies against CEBPB (Cell Signaling), TNF-α(Abcam), p-STAT6 (Cell Signaling), p-JAK1 (Cell Signaling), and β-actin (Santa Cruz). HRP-conjugated secondary antibodies were used for detection, and protein bands were visualized using

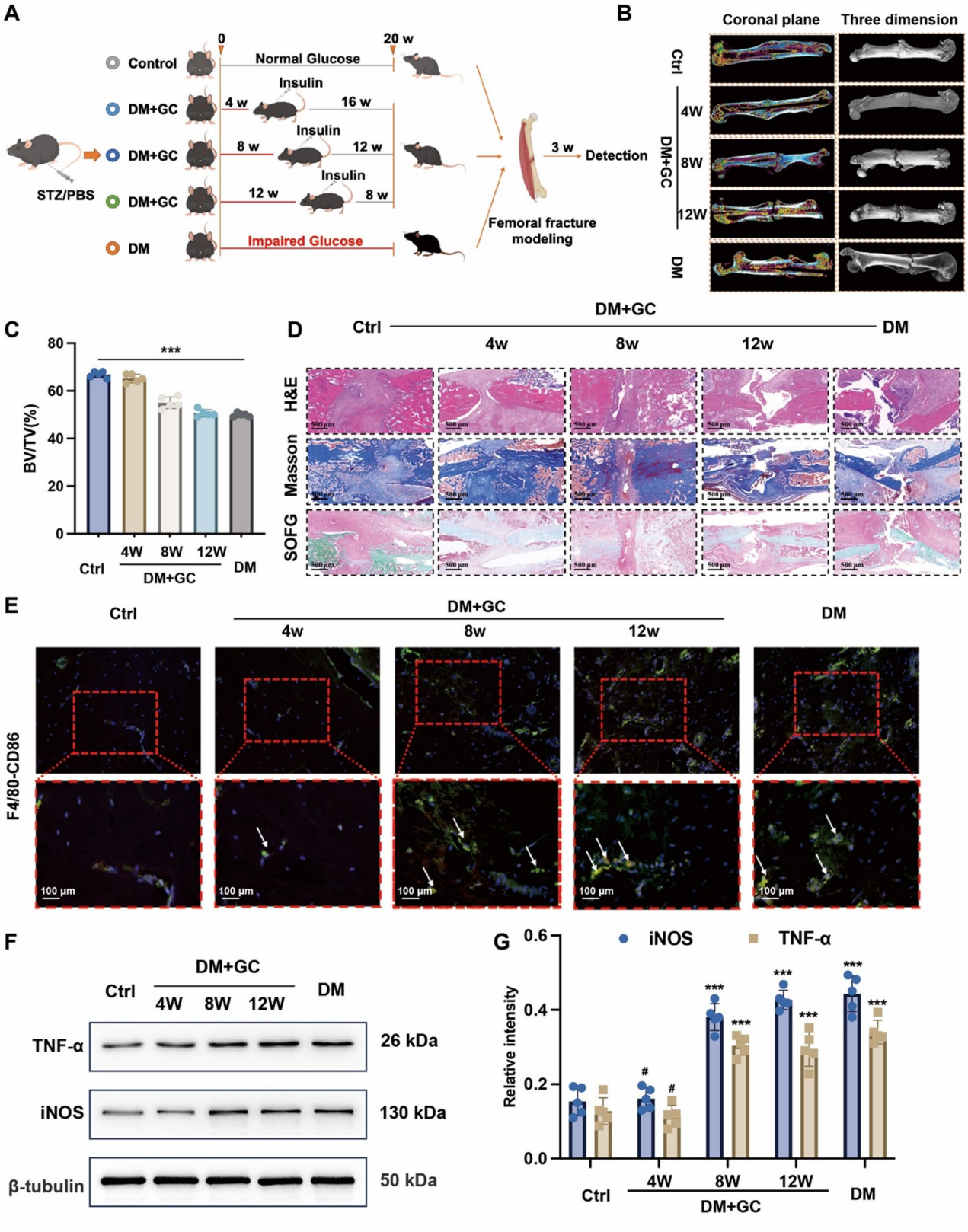

Fig. 1 (See legend on next page.)

(See figure on previous page.)

Fig. 1 BMDMs are involved in sustained effects of hyperglycemia on fracture healing even after glucose normalization. **A** Experimental design. **B**-**C** Micro-CT and quantitative analysis revealed a larger fracture gap and smaller callus volume in DM and DM/GC groups after 8 weeks of hyperglycemia. **D** Histological examination of H&E, Masson's trichrome, and Safranin O-fast green staining showed impaired healing at the fracture site in both DM and DM/GC groups exposed to hyperglycemia for over 8 weeks. **E** Immunofluorescence staining revealed a significant increase in M1 macrophages in the DM and DM/GC groups in response to sustained hyperglycemia compared to the Ctrl group. (**F**-**G**) Western blot analysis showed increased levels of pro-inflammatory cytokines in the DM and DM/GC groups with prolonged hyperglycemia exposure. (Full-length blots/gels are presented in Supplementary Fig. 1 A). The data were analyzed using one-way ANOVA, followed by Tukey's post-hoc test (C, F). Data are presented as the mean ± SD, $^{\#}p > 0.05$, $^{*}p < 0.05$, $^{**}p < 0.01$, $^{***}p < 0.001$

ECL chemiluminescence substrate. Densitometric analysis was performed using ImageJ software.

Exosome isolation and SiRNA delivery

Exosomes were isolated from serum using ultracentrifugation as previously described. Briefly, serum was first centrifuged at 3000×g for 10 min to remove cell debris. The supernatant was then transferred to ultracentrifuge tubes and subjected to high-speed centrifugation at 100,000×g for 2 h to isolate exosomes. The exosome pellet was resuspended in PBS and stored at −80 °C until further use. For exosome-mediated siRNA delivery, CEBPB-specific siRNA (si-CEBPB) was loaded into exosomes via calcium-mediated transfection. The procedure was performed according to the manufacturer's instructions, with modifications to improve the transfection efficiency. After siRNA loading, the exosome preparation was incubated for 24 h, after which the exosomes were collected and their efficiency confirmed by qPCR and western blot analysis for CEBPB expression.

Immunohistochemistry assay

Bone specimens from three patient groups were collected during surgery, and immunohistochemical analysis was subsequently conducted. Briefly, 4 μm paraffin-embedded tissue sections were prepared to evaluate the expression of the CEBPB protein. The specimens were fixed in formaldehyde and embedded in paraffin, with control tissues processed in parallel. Decalcification was performed using 10% EDTA (pH 7.4) at 4 °C for 4 weeks. Tissue sections were cut into 4 μm slices, deparaffinized in xylene for 25 min, and sequentially rehydrated in graded ethanol solutions (100%, 95%, 80%, and 70%) for 5 min each. Antigen retrieval was performed using a 0.01 M citric acid buffer heated in a microwave for 3 min at high power, followed by 10 min at low power. Endogenous peroxidase activity was quenched by incubating the slides with 3% hydrogen peroxide (H_2O_2) at room temperature. After rinsing in PBS, the slides were blocked with 10% goat serum for 30 min. Rabbit anti-human CEBPB antibody (1:200; Millipore, USA) was applied, and the sections were incubated overnight at 4 °C. Following three washes in PBS, HRP-conjugated secondary antibodies were added, and the slides were incubated at room temperature for 30 min.

Micro-CT and histological analysis

After 3 weeks post-operation, the femurs were collected and fixed in 4% paraformaldehyde overnight. Then, micro-CT (SkyScan1276, Bruker, Belgium) was used to assess new bone formation in fracture sites at a resolution of 40 μm with 63 kV and 200 μA. In addition, 3D structures and bone volume/total volume (BV/TV) of the fracture sites were used to evaluate bone regeneration. To further evaluate osteogenesis in fracture sites, Masson, H&E and safranin O-fast green staining were performed. To assess the immunomodulation of BMDMs in the fracture microenvironment, immunofluorescence staining was performed with CD86 and CD206. Finally, samples were observed via a microscope.

Statistical analysis

All data are expressed as the mean ± standard deviation (SD). Statistical analysis was performed using GraphPad Prism software. The data were analyzed using one-way ANOVA, followed by Tukey's post-hoc test, or Student's t-test where appropriate. Differences were considered statistically significant at $p < 0.05$.

Results

BMDMs are involved in the sustained effects of hyperglycemia on fracture even after glucose normalization in diabetic rats

As presented in Fig. 1A, to investigate whether BMDMs are involved in the sustained effects of hyperglycemia on fracture even after glucose normalization in diabetic mice, animals were divided into control group (Ctrl), diabetic group (DM), and diabetic group with glucose control (DM/GC). The fracture repair at the fracture site was evaluated through micro-CT and histological examinations. The micro-CT studies revealed a fracture gap and a smaller callus volume happened in DM and DM/GC with hyperglycemia exposure for more than 8 weeks when compared with other groups (Fig. 1B). Quantitative analysis of micro-CT data demonstrated that the bone volume/total volume (BV/TV) values (Fig. 1C). As shown in Fig. 1D, histology images for H&E, Masson, safranin O-fast green displayed that there was a visible hindrance in the fracture site in DM and DM/GC with hyperglycemia exposure for more than 8 weeks compared with other groups. To further confirm the observed changes of BMDMs subtypes, immunofluorescence detection

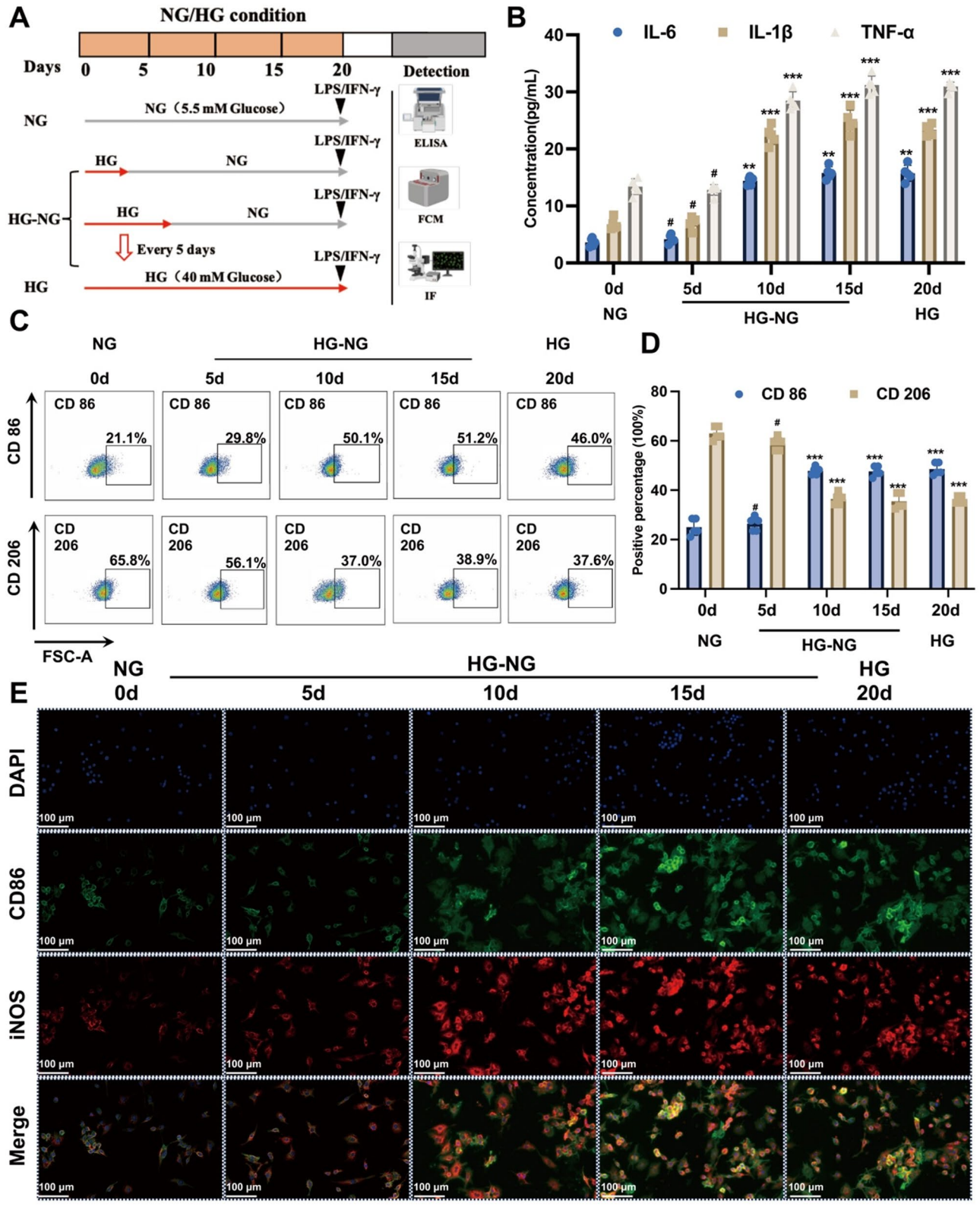

Fig. 2 (See legend on next page.)

(See figure on previous page.)

Fig. 2 Metabolic memory and inflammatory profiles in BMDMs induced by transient hyperglycemia. **A** Experimental design: BMDMs were cultured in HG for varying durations followed by return to NG conditions for an additional day. **B** ELISA results showed significantly increased levels of IL-1β, IL-6, TNF-α in the HG/NG group after 10 days of HG exposure compared to the NG group. **C**-**D** Flow cytometry analysis revealed a significantly higher proportion of M1 macrophages in the HG/NG group exposed to HG for more than 10 days, while the NG and short HG exposure groups (5 days) had a higher proportion of M2 macrophages compared to the NG group. **E** Immunofluorescence analysis confirmed an increase in CD86 and iNOS-positive cells in BMDMs with prolonged HG exposure. The data were analyzed using one-way ANOVA, followed by Tukey's post-hoc test (**B**, **D**). All experiments were repeated three times and shown are representative data, $^{\#}p > 0.05$, $^{*}p < 0.05$, $^{**}p < 0.01$, $^{***}p < 0.001$

was performed. The amount of M1 BMDMs (F4/80-CD86) in DM and DM/GC with hyperglycemia exposure 8 weeks was significantly higher than that in other groups (Fig. 1E). In addition, immunofluorescence staining of CD206 revealed a marked reduction in fluorescence intensity after 8 weeks of hyperglycemia exposure, indicating suppressed M2 polarization (Supplementary Fig. 2B-C). Furthermore, changes in the content of cytokines, including iNOS and TNF-α were measured via western blot. As is displayed in Fig. 1F-G, compared to other groups, the content of pro-inflammatory cytokines increased in DM and DM/GC with hyperglycemia exposure for more than 8 weeks. Altogether, all these data indicate that BMDMs are involved in the sustained effects of hyperglycemia on fracture even after glucose normalization in diabetic mice.

Evidence of hyperglycaemia-induced metabolic memory in BMDMs

As is displayed in Fig. 2A, to simulate the transient hyperglycemia conditions in vitro, BMDMs in HG/NG group were first incubated BMDMs in HG for 5, 10, 15 days and then returned to the NG concentration until 20 days; BMDMs cultured in NG were used to simulate physiological glucose levels, and cultured in HG alone were used to characterize DM without tight glucose control. To investigate whether transient hyperglycemia induces metabolic memory and downstream pro-inflammatory profiles in BMDMs, we performed Seahorse extracellular flux analysis to assess their metabolic status. Following 10- and 15-day exposure to HG, cells exhibited a marked increase in ECAR compared to control groups, indicating enhanced glycolytic activity. In contrast, OCR remained largely unchanged, suggesting minimal effects on mitochondrial respiration. Notably, this elevated glycolysis persisted even after cells were returned to normoglycemic conditions, supporting the existence of a hyperglycemia-induced metabolic memory phenotype (Supplementary Fig. 2D-E). Consistently, as shown in Fig. 2B, the results presented that protein levels of IL-1β, IL-6 and TNF-α were markedly increased in HG/NG group with HG exposure for more than 10 days, compared to NG group. To further evaluate the effect of the transient hyperglycemia exposure on BMDMs, flow cytometry was used to evaluate macrophage polarization. M1 macrophages were defined as $F4/80^{+}$ and $CD86^{+,}$ while M2 macrophages were defined as $F4/80^{+}$ and $CD206^{+}$ [25]. The M1 macrophage population in HG/NG group with HG exposure for more than 10 days was also significantly higher than other groups. In contrast, NG group and HG/NG group with HG exposure for 5 days had significantly more M2 macrophages than HG/NG group with HG exposure for 10, 15, and 20 days (Fig. 2C-D). Moreover, further analysis of immunofluorescence detection offered a similar result that a large number of CD86 and iNOS-positive cells were observed in BMDMs with HG exposure for more than 10 days (Fig. 2E). Therefore, all these data suggest that BMDMs can be induced in a metabolic memory via HG exposure for more than 10 days, persistently maintaining pro-inflammatory state even after glucose normalization.

BMDMs in hyperglycaemia-induced metabolic memory attenuate the process of osteogenesis and angiogenesis

We next determined the effects of BMDMs in hyperglycaemia-induced metabolic memory on the osteogenesis of BMSCs and the angiogenesis of HUVECs. BMDMs were divided into NG group, HG group, and MM group; and BMDMs in MM group is were first incubated in hyperglycaemia for 10 days and then returned the normal glucose concentration. The osteogenesis of BMSCs in the co-culture medium from BMDMs was evaluated by ALP staining, ARS staining, western blot, and immunofluorescence staining. The photographs shown in Fig. 3A indicate that the co-culture medium from BMDMs in MM and HG groups displayed the less intense ALP and ARS staining when compared with the NG group. And OD values were measured to quantitatively evaluate the ALP and ARS staining; the results were consistent with those from light microscopy (Fig. 3B). In addition, the expression of osteogenic proteins, such as Runx2 and OCN, was evaluated to validate the osteogenic differentiation of BMSCs in the co-culture medium from BMDMs in different groups. As exhibited in Fig. 3C-D, significantly down-regulated expression of these proteins was measured in MM and HG groups relative to that in the NG group. Furthermore, Immunofluorescence staining also confirmed that BMSCs cultured in the co-culture medium from BMDMs in MM and HG groups expressed lower levels of Runx2 and OPN. All those results demonstrate that BMDM in hyperglycaemia-induced metabolic memory attenuates the osteogenic differentiation of BMSCs. To assess the effect of the co-culture medium from BMDMs in different groups on angiogenesis, many

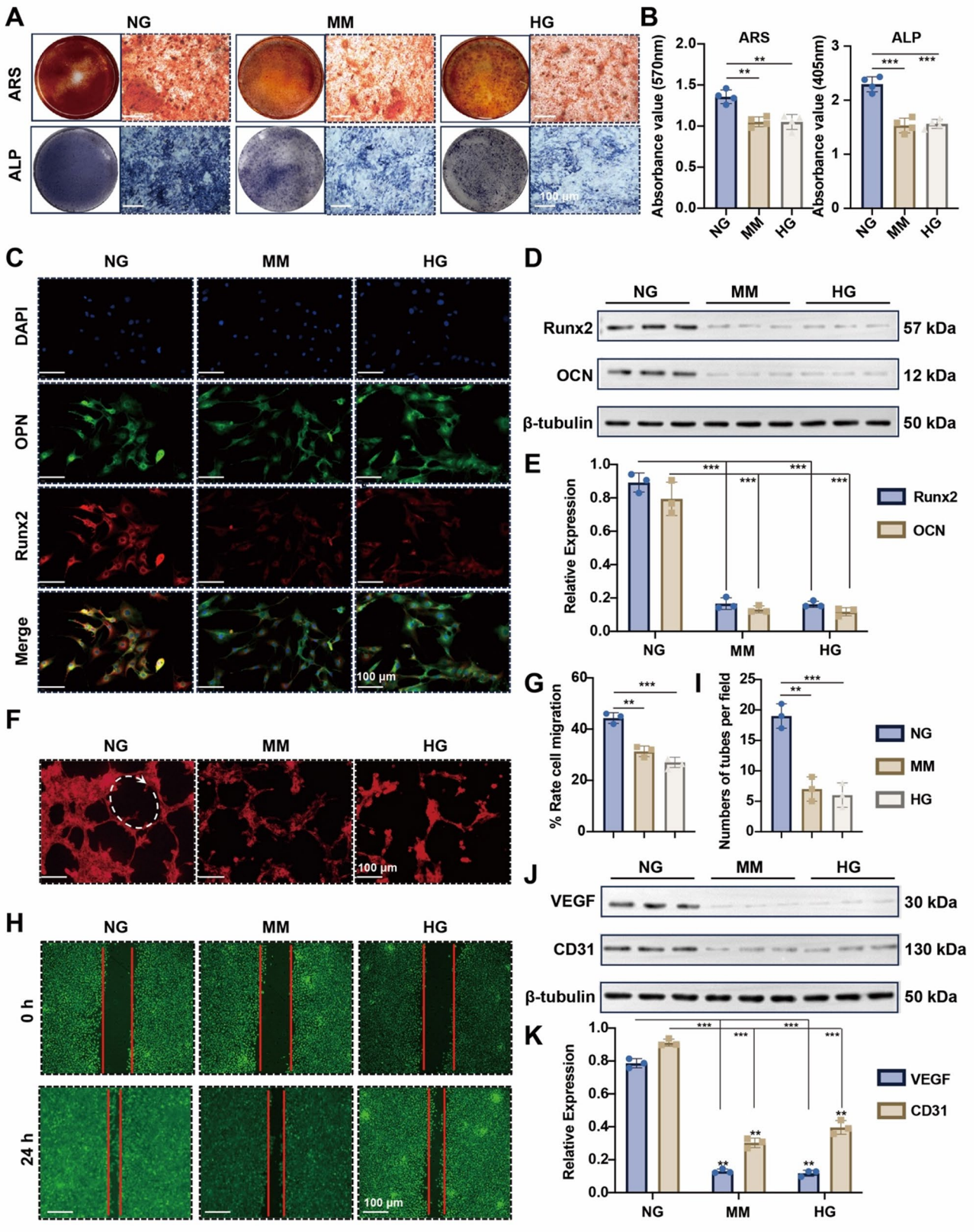

Fig. 3 (See legend on next page.)

(See figure on previous page.)

Fig. 3 Effects of BMDMs in hyperglycemia-induced metabolic memory on osteogenesis and angiogenesis. **A** ALP and ARS staining of BMSCs co-cultured with BMDMs from NG, HG, and MM groups. **B** The statistical data of Alizarin red staining and ALP staining. **C**-**D** Western blot analysis revealed significantly downregulated osteogenic markers Runx2 and OCN in the MM and HG groups compared to the NG group. (Full-length blots/gels are presented in Supplementary Fig. 1B). **E** Immunofluorescence staining showed lower expression of Runx2 and OPN in BMSCs cultured with medium from MM and HG BMDMs. **F**-**G** Representative fluorescence images and quantitative analysis of HUVEC tube formation after the cells were co-cultured with BMDMs in different groups. **H**-**I** Migration ability of HUVECs and quantitative analysis in NG, HG, and MM groups. **J**-**K** Western blotting analysis of VEGF and CD31. (Full-length blots/gels are presented in Supplementary Fig. 1 C). The data were analyzed using one-way ANOVA, followed by Tukey's post-hoc test (**B**, **E**, **G**, **I**, **K**). All experiments were repeated three times and shown are representative data, $^{\#}p > 0.05$, $^{*}p < 0.05$, $^{**}p < 0.01$, $^{***}p < 0.001$

biological function assessments, such as HUVEC tube formation, scratch wound healing assays and western blot. As shown in Fig. 3F-I, the co-culture medium in MM and HG groups impaired the migration and tube formation of HUVECs. These changes are very harmful to angiogenesis during fracture healing and repair. Moreover, as shown by Western blot, the angiogenesis-related genes, including VEGF and CD31 were downregulated in MM and HG groups in comparison with NG group. These data indicate that BMDMs in hyperglycaemia-induced metabolic memory may cause a harmful microenvironment for fracture healing and repair.

Transcriptional analysis shows that inflammatory factors are associated with the hyperglycaemia-induced metabolic memory in BMDMs

RNA-seq was used to conduct gene transcription analysis between BMDMs in MM and NG groups. Principal component analyses (PCA) of the whole-genome expression profiles showed that BMDMs in MM group were separated from that in NG group (Fig. 4A). Compared to NG group, BMDMs in MM group showed 2114 up-regulated genes and 1505 down-regulated genes (Fig. 4B). These comparisons presented that the conversion of BMDMs in MM to that in NG is associated with large changes in gene expression. Then, the function of differentially expressed genes (DEGs) between BMDMs in different groups was further investigated. Gene set enrichment analysis (GSEA) revealed that processes associated with IL-6 production, inflammatory response, innate immune response and regulation of NF-κB response were activated in MM group; Similarly, signaling pathway associated with NOD-like receptor signaling pathway, TNF signaling pathway, HIF-1α signaling pathway and AGE-RAGE signaling pathway in diabetic complications were inhibited in NG group and activated in MM group (Fig. 4C). Among them, inflammatory factors were significantly up-regulated in MM group and down-regulated in NG group, including interleukins (IL-6, IL-1α, IL-1β, IL-7, etc.), chemokines (TNF, HIF-1α, CCL-2, CXCL-2, etc.), proteases and regulators (MMP-3, MMP-9, USP-25, etc.) (Fig. 4D). Since the expression of various proinflammatory factor genes were associated with BMDMs in MM group, it's important to find their underlying mechanism.

Integrated analysis of RNA-seq and ATAC-seq of BMDMs in hyperglycaemia-induced metabolic memory

Previously we investigated the difference of mRNA expression profile between MM and NG groups through RNA-seq. To investigate whether the transcriptional changes of inflammatory factors observed above were attributed to the dynamic alterations in chromatin structure and the epigenetic code that affected the accessibility to cis-regulatory elements for transcription, we performed integrative RNA-Seq and ATAC-Seq analyses. As expected, the majority of peaks called were located near a transcription start site (TSS) for all libraries (Fig. 5A). As we have shown above, 210 genes with both increased chromatin accessibility and up-regulated mRNA expression were identified; and 132 have both decreased chromatin accessibility and down-regulated mRNA expression (Fig. 5B). Next, we made a correlation analysis of the expression levels and chromatin accessibility of overlapping genes and detected a significant positive correlation between the differential gene expression and differential ATAC-seq signal ($R = 0.8$; Fig. 5C). We also made a gene-based heatmap using RNA expression level and ATAC-seq signal and confirmed the reproducible pattern; in addition, the results showed that the increased differential accessibility regions were associated with upregulated genes and that the decreased differential accessibility regions were associated with downregulated genes (Fig. 5D). Moreover, KEGG analysis of these 342 genes suggested that multiple terms were changed in especially for inflammatory related pathways, such as TNF signaling pathway, TGF-β signaling pathway, HIF-1α signaling pathway. To identify candidate transcription factors binding to the gained peak regions and potentially regulating inflammation-related gene expression, motif analysis was performed. The top five enriched TF binding motifs with gene expression in MM and NG groups were shown in Fig. 5E. Through an analysis of TFs in RNA-seq, five TFs were obtained and displayed in the heatmap of mRNA expression; among them, BATF and CEBPB were up-regulated in MM groups (Fig. 5F). And as shown by western blot, a significantly increased expression in CEBPB was observed in MM group, but the expression of BATF in MM group had no significant difference from that in NG group (Fig. 5G-H). To further validate our findings, we collected bone tissue samples from non-diabetic individuals, poorly controlled diabetic

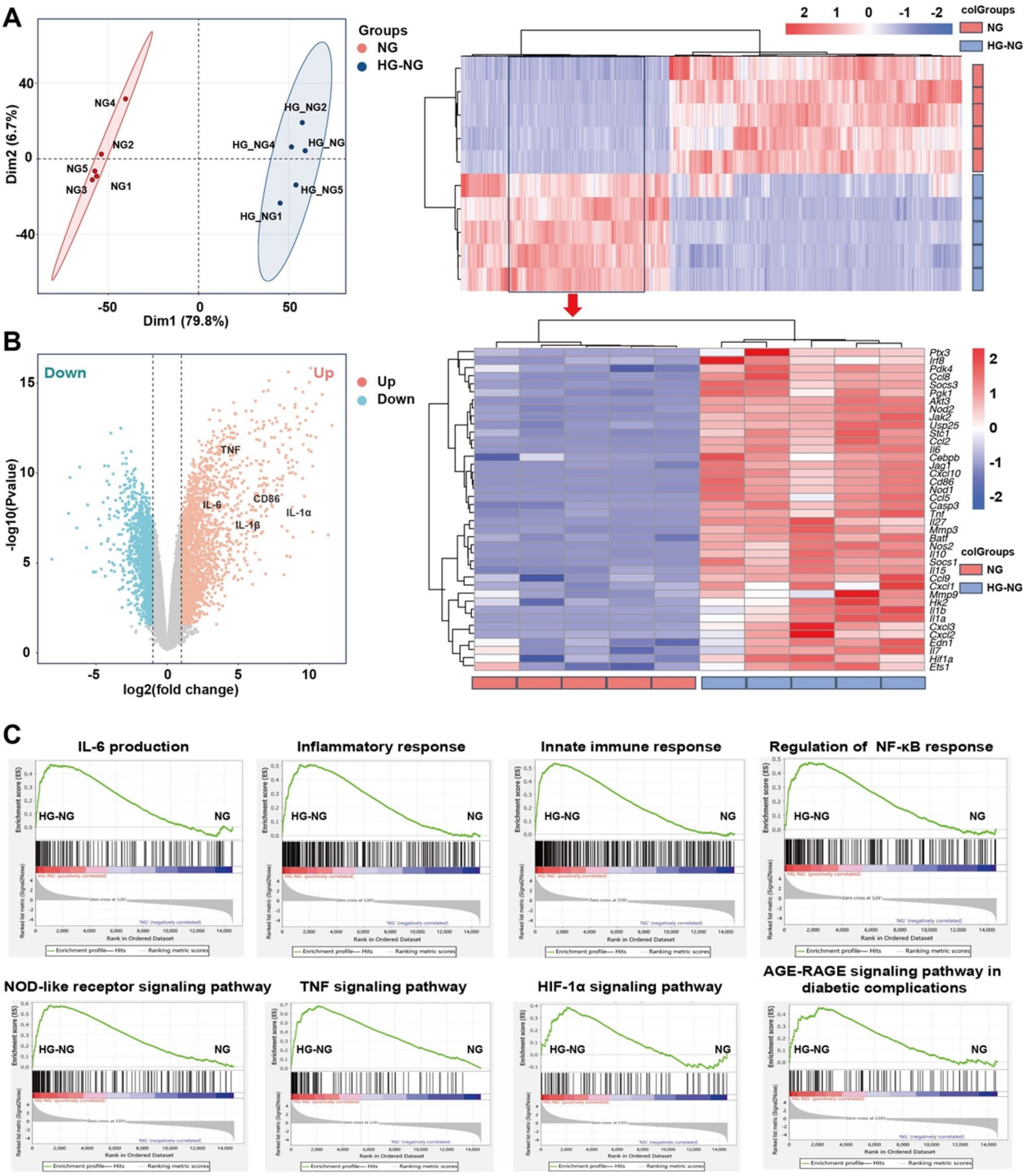

Fig. 4 Transcriptional analysis of inflammatory factors in BMDMs with hyperglycemia-induced metabolic memory. **A** PCA of RNA-seq data showed a clear separation between BMDMs in the MM and NG groups. **B** Volcano plot of genes expressed differently in two groups. **C** GSEA indicated activation of processes related to IL-6 production, inflammatory response, and NF-κB regulation in the MM group, while pathways such as NOD-like receptor signaling, TNF signaling, and AGE-RAGE signaling were activated in MM and suppressed in the NG group. **D** The heat map showed that inflammatory factors, including interleukins (IL-6, IL-1β), chemokines (TNF, CCL-2), and proteases (MMP-3, MMP-9), were significantly up-regulated in the MM group

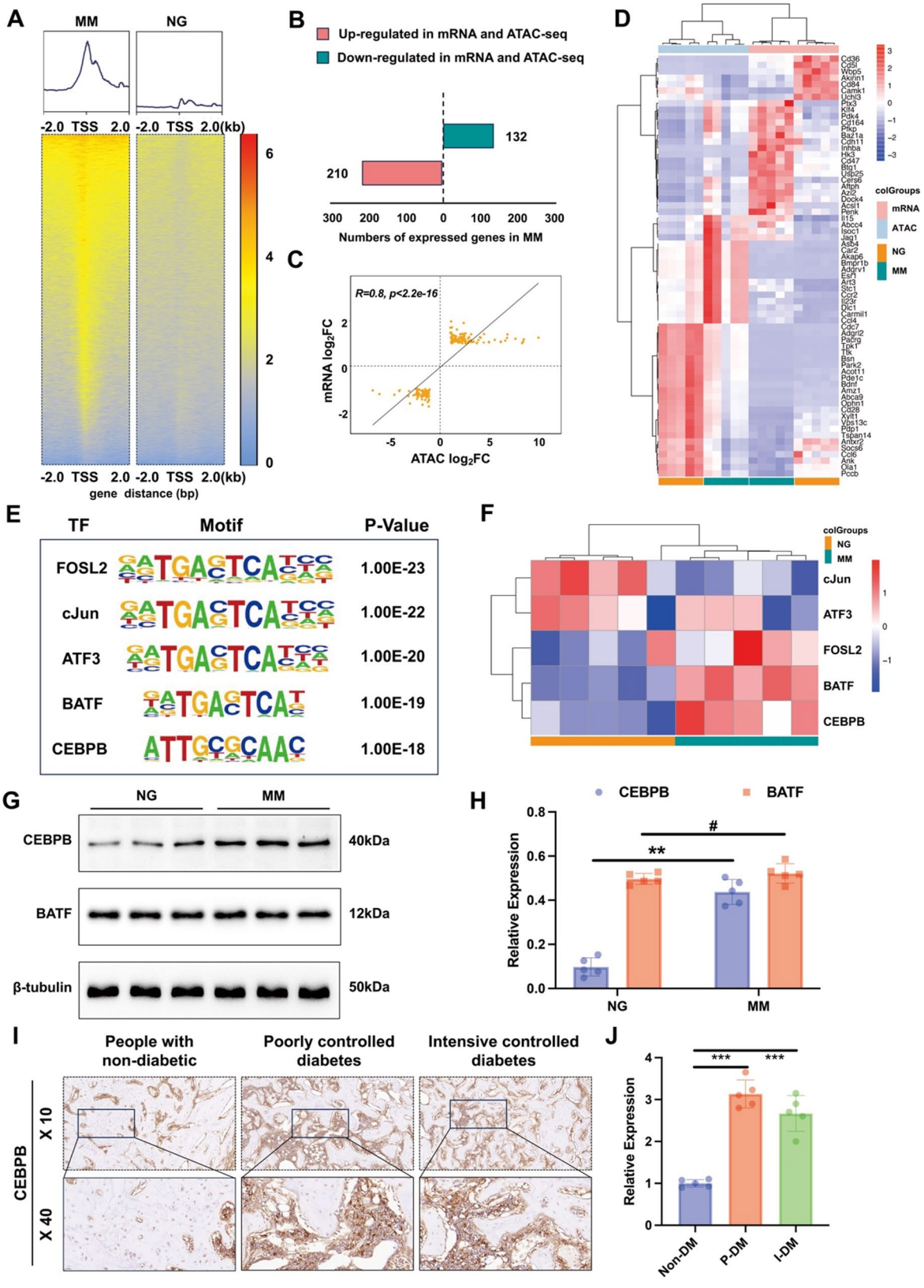

Fig. 5 (See legend on next page.)

(See figure on previous page.)

Fig. 5 Integrated analysis of RNA-seq and ATAC-seq in BMDMs with hyperglycemia-induced metabolic memory. **A** Distribution of ATAC-seq peaks around TSS across all libraries. **B** Identification of 210 genes with increased chromatin accessibility and up-regulated mRNA expression, and 132 genes with decreased chromatin accessibility and down-regulated mRNA expression. **C** A significant positive correlation between differential gene expression and differential ATAC-seq signals. **D** Heatmap showing a reproducible pattern of increased chromatin accessibility correlating with up-regulated genes and decreased accessibility with down-regulated genes. **E** Motif analysis identified top-enriched TF binding motifs in gained peak regions, suggesting regulation of inflammatory gene expression. **F** Heatmap showing upregulation of BATF and CEBPB in MM group. **G**-**H** Western blot analysis showing increased CEBPB expression in the MM group, while BATF expression remained unchanged. (Full-length blots/gels are presented in Supplementary Fig. 1D). **I**-**J** Immunohistochemical detection of CEBPB in people with non-diabetic, poorly controlled diabetes and intensively controlled diabetes. The data were analyzed using one-way ANOVA, followed by Tukey's post-hoc test **J** and Student's t-test (**H**). Data are presented as the mean ± SD. $^{\#}p > 0.05$, $^{*}p < 0.05$, $^{**}p < 0.01$, $^{***}p < 0.001$

patients, and intensively controlled diabetic patients for immunohistochemical detection of CEBPB. The results indicated that, compared to non-diabetic patients, the expression levels of CEBPB in bone tissue were significantly increased in both well-controlled and poorly controlled diabetic patients (Fig. 5I-J). Therefore, our results indicate that increased expression of CEBPB may play an important role in the existence of metabolic memory phenomenon and its negative effect on fracture healing in diabetes.

siRNA-mediated knockdown of CEBPB partially reverses hyperglycaemia-induced metabolic memory in BMDMs and its adverse effect on osteogenesis and angiogenesis

Numerous studies have reported that CEBPB plays a critical role in regulating the function of macrophages. And our aforementioned data demonstrated that increasing the expression of CEBPB is associated with BMDMs in hyperglycaemia-induced metabolic memory. To get more insight into whether silencing CEBPB could reverse hyperglycaemia-induced metabolic memory in BMDMs, we utilized siRNA to silence CEBPB. Indeed, decreased CEBPB, TNF-α and increased Arg-1 were observed in MM group upon CEBPB silencing treatment (Fig. 6A-D). We then determined the effects of silencing CEBPB on the osteogenesis of BMSCs or the angiogenesis of ECs in MM group respectively. The osteogenesis of BMSCs in the co-culture medium from BMDMs treated by CEBPB silencing in MM group was assessed via ALP staining, ARS staining and immunofluorescence staining. As shown by ALP staining and Alizarin red staining, the proportion of mineralization was increased by si-CEBPB when compared with the control group (Fig. 6E-F). Migration ability of HUVECs and quantitative analysis in two groups revealed that silencing CEBPB promotes the migration ability of HUVECs (Fig. 6G-H). And immunofluorescence staining also showed that BMSCs cultured in the co-culture medium from BMDMs treated by CEBPB silencing in MM group expressed higher levels of Runx2 and OPN (Fig. 6I). In the tube formation assay, more branches and intact tubules were observed in the silencing CEBPB of BMDMs (Fig. 6J-K). These demonstrated that siRNA-mediated knockdown of CEBPB partially reverses hyperglycaemia-induced metabolic memory in BMDMs and its adverse effect on osteogenesis and angiogenesis.

CEBPB is associated with JAK1/STAT6 pathway when BMDMs in hyperglycaemia-induced metabolic memory and delivering si-CEBPB to fracture sites using exosomes can enhance diabetic fracture healing

The canonical JAK1/STAT6 pathway plays a key role in macrophage polarization. Upon activation by external stimuli, the JAK1 phosphorylates STAT6, leading to its dimerization and translocation into the nucleus. There, STAT6 induces the expression of genes involved in tissue repair, anti-inflammatory responses which promote M2 macrophage polarization. And extensive literature has detailed that CEBPB inhibits JAK1-STAT6 pathway activation, leading to impaired M2 polarization of macrophages, causing a large number of macrophages to remain in the M1 phenotype. Western blot analysis revealed low expression of p-STAT6, p-JAK1 and JAK1 in MM group when compared with NG group. Meanwhile, si-CEBPB enhanced the expression of p-STAT6, p-JAK1 and JAK1, suggesting that CEBPB might be associated with JAK1/STAT6 pathway when BMDMs in hyperglycaemia-induced metabolic memory (Fig. 7A-F). And as shown in Fig. 7G, a large number of BMDMs expressing the M1 marker CD86 and iNOS were observed in the metabolic memory group; however, this phenomenon can be reversed by si-CEBPB. Based on the fact that exosomes efficiently deliver siRNA in vivo, si-CEBPB was loaded into serum exosomes using modified calcium-mediated transfection, as described in previous report. To investigate whether the exosomes-delivered si-CEBPB improve fracture healing, we performed the following experiments. After the establishment of the diabetic fracture model, PBS (Control), control siRNA/EXOs (Exo@Cont-siRNA) or siCEBPB/EXOs (Exo@si-CEBPB) were administered into fracture sites every two days. We further observed a markedly decreased fracture gap and a larger callus volume in Exo@si-CEBPB group compared with Control and Exo@Cont-siRNA group (Fig. 7H-I). Further analysis of BV/TV offered a similar result (Fig. 7J).

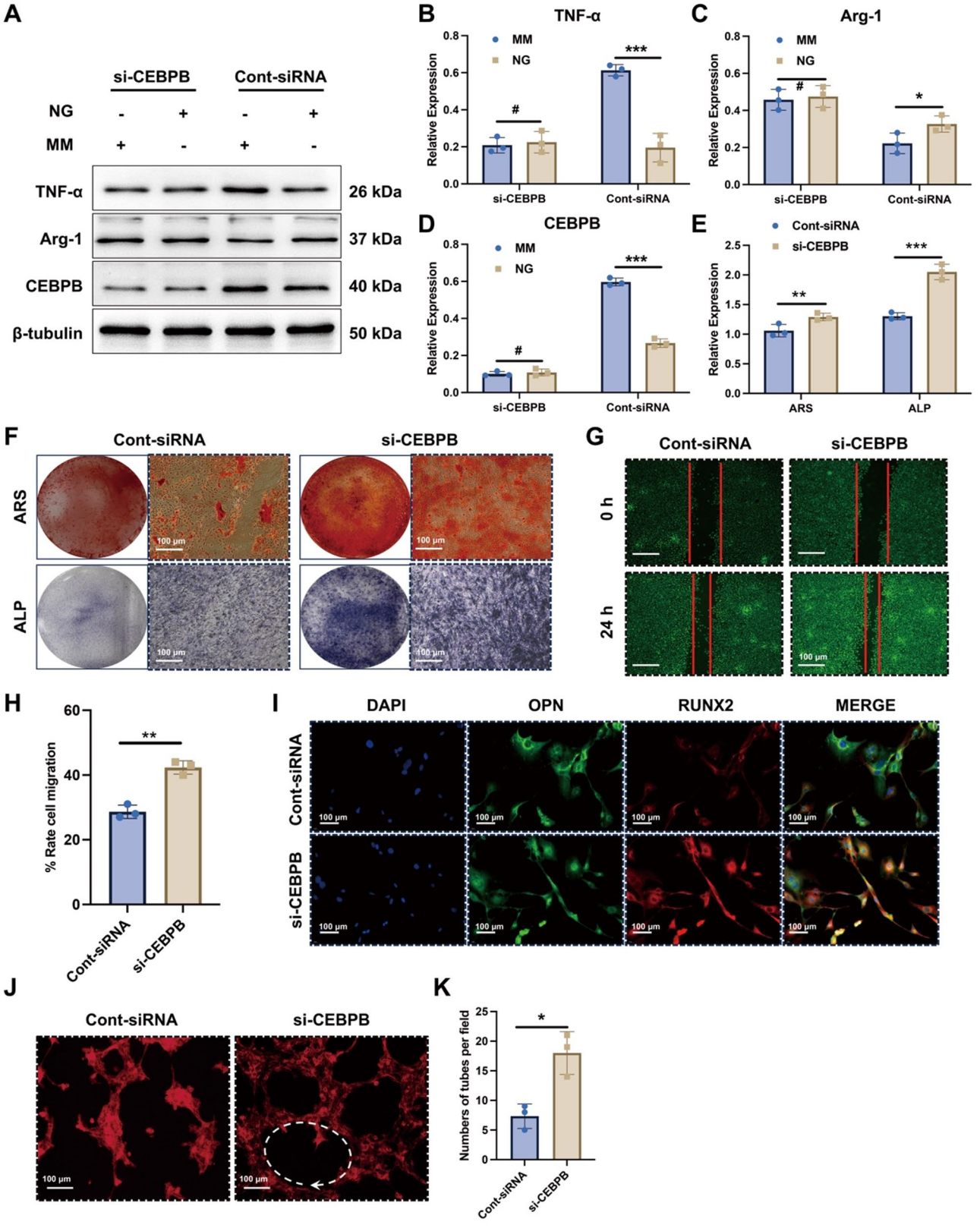

Fig. 6 (See legend on next page.)

(See figure on previous page.)

Fig. 6 siRNA-mediated knockdown of CEBPB partially reverses hyperglycemia-induced metabolic memory in BMDMs. **A**-**D** Western blot analysis revealed that silencing CEBPB in MM group reduced the expression of CEBPB and TNF-α, while increasing the anti-inflammatory marker Arg-1. (Full-length blots/gels are presented in Supplementary Fig. 1E). **E**-**F** ALP and ARS staining revealed enhanced mineralization in BMSCs co-cultured with BMDMs treated with si-CEBPB in the MM group. **G** Immunofluorescence staining showed increased expression of osteogenic markers Runx2 and OPN in BMSCs in the co-culture medium from si-CEBPB-treated BMDMs. **H**-**K** Migration ability and tube formation of HUVECs suggest that silencing CEBPB promotes angiogenesis in the MM group. The data were analyzed using Student's t-test (**B**-**E**, **H**, **K**). Data are presented as the mean ± SD, $^{\#}p > 0.05$, $^{*}p < 0.05$, $^{**}p < 0.01$, $^{***}p < 0.001$

Discussion

The present study investigates the role of hyperglycemia-induced metabolic memory in BMDMs and its detrimental effects on fracture healing in diabetes. Our findings underscore that the persistent pro-inflammatory phenotype of BMDMs, triggered by transient hyperglycemia, plays a crucial role in the delayed fracture healing observed in diabetes. This study highlights the importance of understanding the mechanisms of metabolic memory in macrophages, specifically their impact on osteogenesis and angiogenesis during bone repair in diabetic conditions.

In this study, we show that transient hyperglycemia, even after glucose normalization, results in sustained pro-inflammatory responses in BMDMs, leading to impaired fracture healing. Our findings align with previous studies that have demonstrated the role of metabolic memory in various diabetic complications, including atherosclerosis, nephropathy, and cardiomyopathy [6, 26–28]. In the context of bone repair, it has long been known that diabetes negatively impacts osteogenesis and angiogenesis, and the concept of metabolic memory provides a mechanistic explanation for the persistence of these effects even after blood glucose levels are normalized [29, 30].

The elevated levels of M1 macrophages in the fracture sites of diabetic rats, observed in our study, provide further evidence for the involvement of an altered immune response in metabolic memory. These findings are consistent with the literature, where increased numbers of M1 macrophages have been linked to delayed wound healing and impaired bone repair in diabetes [31, 32]. Macrophage polarization is a critical factor in the regulation of inflammation and tissue repair, with M1 macrophages being pro-inflammatory and M2 macrophages promoting tissue regeneration. The imbalance in macrophage polarization, as shown in our study, disrupts the repair process and may contribute to the pathophysiology of diabetic fracture healing. Given the central role of macrophages in tissue repair, numerous strategies have been developed to modulate macrophage polarization in favor of the M2 phenotype, including the delivery of cytokines such as IL-4, application of metabolic regulators like metformin, and use of immunomodulatory biomaterials [33–35].

Our results indicate that BMDMs in metabolic memory inhibit osteogenesis in BMSCs, as evidenced by reduced alkaline phosphatase activity, alizarin red staining, and lower expression of osteogenic markers such as Runx2 and OCN. This is consistent with our previous studies showing that hyperglycemia impairs osteoblast differentiation and mineralization [11]. The co-culture system used in this study reveals that the pro-inflammatory cytokines secreted by metabolic memory-activated BMDMs hinder the osteogenic differentiation of BMSCs, a key process in bone healing. Moreover, our study demonstrates that BMDMs in metabolic memory also impair angiogenesis, a crucial process in fracture healing. The reduction in endothelial cell migration, tube formation, and downregulation of angiogenesis-related proteins, such as VEGF and CD31, further underscores the negative impact of metabolic memory on the fracture healing process. These findings align with those of earlier studies, which have shown that diabetes impairs angiogenesis, leading to delayed fracture healing [36]. The sustained inflammatory environment created by M1-polarized BMDMs likely contributes to a microenvironment that is less conducive to the formation of new blood vessels, which are essential for supplying nutrients and oxygen to the healing bone.

A major contribution of this study is the identification of CEBPB as a key mediator of metabolic memory in BMDMs. Our results show that CEBPB expression is upregulated in BMDMs exposed to transient hyperglycemia, and this upregulation is associated with a persistent pro-inflammatory phenotype. CEBPB is a transcription factor known to play a critical role in macrophage activation and inflammation [37]. Previous studies have demonstrated that CEBPB regulates the expression of pro-inflammatory cytokines in macrophages and contributes to the pathogenesis of inflammatory diseases [38]. Our data suggest that CEBPB is central to the metabolic memory phenomenon in BMDMs, maintaining an inflammatory state even after glucose levels are normalized.

The significant role of CEBPB in modulating the inflammatory response in BMDMs and its impact on fracture healing is supported by recent literature. Studies have shown that inhibition of CEBPB in macrophages can reduce inflammation and promote tissue repair [39]. Our siRNA-mediated knockdown of CEBPB partially reversed the detrimental effects of metabolic memory on osteogenesis and angiogenesis, providing compelling evidence that targeting CEBPB may be a potential

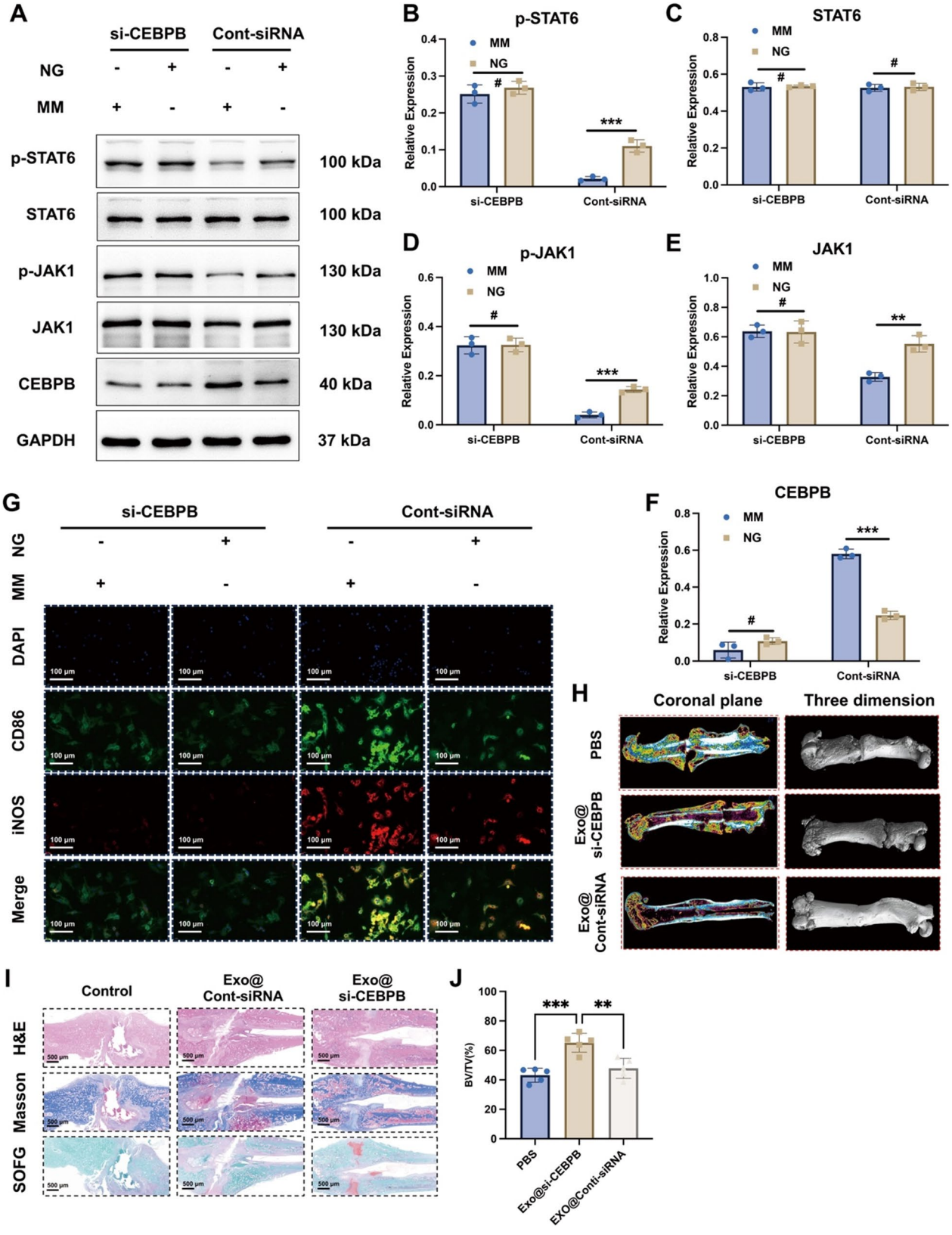

Fig. 7 (See legend on next page.)

(See figure on previous page.)

Fig. 7 CEBPB is associated with the JAK1/STAT6 pathway in BMDMs. **A**-**F** Western blot analysis revealed decreased expression of p-STAT6, p-JAK1, and JAK1 in the MM group compared to the NG group. si-CEBPB treatment restored the expression of these markers. (Full-length blots/gels are presented in Supplementary Fig. 1 F). **G** Immunofluorescence staining showed increased expression of M1 markers CD86 and iNOS in the MM group, which was reversed by si-CEBPB treatment. **H**-**I** micro-CT, H&E, safranin O-fast green staining and Masson's of the femurs showed that exosomes loaded with si-CEBPB (Exo@si-CEBPB) had a significant reduction in fracture gap and increased callus volume compared to other groups. Quantitative analysis of BV/TV also showed enhanced bone healing in the Exo@si-CEBPB group. The data were analyzed using one-way ANOVA, followed by Tukey's post-hoc test **J** and Student's t-test (**B**-**F**). Data are presented as the mean ± SD, $^{\#}p > 0.05$, $^{*}p < 0.05$, $^{**}p < 0.01$, $^{***}p < 0.001$

therapeutic strategy to improve fracture healing in diabetic patients.

Further investigation into the mechanism underlying CEBPB's role in metabolic memory revealed its interaction with the JAK1/STAT6 pathway, which is crucial for macrophage polarization. Our results demonstrate that CEBPB inhibits the activation of the JAK1/STAT6 pathway, thereby preventing the polarization of macrophages toward the M2 phenotype. This finding is consistent with studies showing that M2 macrophages, which promote tissue repair and regeneration, are impaired in diabetic conditions due to disrupted the signaling pathways [40]. By silencing CEBPB, we were able to enhance the activation of the JAK1/STAT6 pathway and shift the macrophage polarization towards the M2 phenotype, thereby improving the healing process.

The therapeutic potential of targeting the JAK1/STAT6 pathway in diabetic fracture healing is supported by recent studies that have highlighted its role in promoting tissue repair and modulating the immune response. For instance, Sun demonstrated that activation of the JAK1/STAT6 pathway promotes M2 polarization and accelerates wound healing in diabetic mice [41]. Our results, showing the beneficial effects of si-CEBPB treatment on fracture healing, suggest that enhancing M2 macrophage polarization via the JAK1/STAT6 pathway could be a promising approach for improving fracture healing in diabetic patients.

An intriguing aspect of our study is the use of exosomes for targeted delivery of siRNA. Exosomes, as natural nanocarriers, have emerged as a promising vehicle for drug delivery, including siRNA, due to their biocompatibility and ability to cross biological barriers [42]. In this study, exosome-mediated delivery of si-CEBPB significantly improved fracture healing in diabetic rats, providing a potential new therapeutic approach for treating diabetic bone fractures. This finding is in line with recent studies exploring the use of exosomes to deliver therapeutic molecules in various disease models, including diabetic fracture healing [43].

Conclusions

In summary, our study demonstrates that BMDMs play a pivotal role in the metabolic memory phenomenon in diabetic fracture healing. The sustained pro-inflammatory state induced by transient hyperglycemia contributes to impaired osteogenesis and angiogenesis, resulting in delayed fracture healing. CEBPB is identified as a key regulator of this process, and targeting CEBPB using siRNA or modulating the JAK1/STAT6 pathway offers potential therapeutic strategies. Additionally, exosome-mediated siRNA delivery holds promise as an innovative approach to enhance fracture healing in diabetic patients.

Abbreviations

BMDMs	Bone marrow-derived macrophages
DM	Diabetes mellitus
DM/GC	Diabetic with glucose control
BV/TV	Bone volume/total volume
HG	High glucose
NG	Normal glucose
BMSCs	Bone marrow mesenchymal stem cells
HUVECs	Human umbilical vein endothelial cells
ALP	Alkaline phosphatase
ARS	Alizarin red staining
PCA	Principal component analysis
DEGs	Differentially expressed genes
GSEA	Gene set enrichment analysis
GO	Gene ontology
KEGG	Kyoto Encyclopedia of Genes and Genomes
HbA1c	Hemoglobin A1c
ANOVA	Analysis of variance

Supplementary Information

The online version contains supplementary material available at https://doi.org/10.1186/s13287-025-04677-9.

Supplementary Material 1

Supplementary Material 2

Supplementary Material 3

Supplementary Material 4

Acknowledgements

We appreciate all the patients who provided samples. The authors declare that they have not used AI-generated work in this manuscript.

Author contributions

Dong Zhang: Conceptualization, Methodology, Software, Validation, Formal analysis, Investigation, Writing, Funding acquisition. Changjiang Liu: Conceptualization, Methodology, Software, Validation, Formal analysis, Investigation, Writing. Ying Yuan: Methodology, Data curation. Junwei Su: Methodology, Investigation. Zheng Wang: Methodology, Software. Chao Jian: Conceptualization, Writing - Review & Editing, Supervision. Aixi Yu: Original Draft, Writing - Review & Editing, Supervision.

Funding

This work was supported by grants from the Science and Technology Innovation Cultivation Fund of Zhongnan Hospital of Wuhan University (CXPY2023028), Excellent Doctor Fund Project of Zhongnan Hospital of Wuhan University (ZNYB2022015), Natural Science Foundation of Hubei Province (2024AFD167), the China Postdoctoral Science Foundation (2023M742701).

Data availability
The datasets generated and/or analyzed during the current study are available from the corresponding author upon reasonable request. All raw RNA-seq and ATAC-seq data supporting the findings of this study are provided in the Supplementary Files.

Declarations

Ethics approval and consent to participate
All of the animal experiments performed in this research were approved by the Ethics Committee of Zhongnan Hospital of Wuhan University (Approval Number: WP20220475; Title: Research on the Mechanism of Metabolic Memory of Bone Marrow Macrophages in the Healing of Diabetic Fractures; Date: April 15 st, 2022). The human studies were reviewed and approved by the Medical Ethics Committee for Clinical Research at Zhongnan Hospital (Approval Number: 20210007; Title: Research on the Mechanism of Fracture Healing in Diabetes; Date: January 1 st, 2021). Written informed consent was obtained from all participants involved in the study. Written informed consent was obtained from the patient for publication of this case report and accompanying images. A copy of the written consent is available for review by the Editor-in-Chief of this journal on request. Our manuscript is reported following the ARRIVE guidelines.

Consent for publication
All the authors have consented to publication.

Competing interests
The authors declare that they have no known competing financial interests or personal relationships that could have influenced the work reported in this study.

Received: 23 May 2025 / Accepted: 12 September 2025
Published online: 14 October 2025

References

1. Hossain MJ, Al-Mamun M, Islam MR. Diabetes mellitus, the fastest growing global public health concern: early detection should be focused. Health Sci Rep. 2024;7(3):e2004.
2. Global regional, and national burden of diabetes. From 1990 to 2021, with projections of prevalence to 2050: a systematic analysis for the global burden of disease study 2021. Lancet. 2023;402(10397):203–34.
3. Fullerton B, Jeitler K, Seitz M, Horvath K, Berghold A, Siebenhofer A. Intensive glucose control versus conventional glucose control for type 1 diabetes mellitus. Cochrane Database Syst Rev. 2014;2014(2):Cd009122.
4. Zhao J, Yang S, Shu B, Chen L, Yang R, Xu Y, et al. Transient high glucose causes persistent vascular dysfunction and delayed wound healing by the DNMT1-mediated Ang-1/NF-κB pathway. J Invest Dermatol. 2021;141(6):1573–84.
5. Siebel AL, Fernandez AZ, El-Osta A. Glycemic memory associated epigenetic changes. Biochem Pharmacol. 2010;80(12):1853–9.
6. Dong H, Sun Y, Nie L, Cui A, Zhao P, Leung WK, et al. Metabolic memory: mechanisms and diseases. Signal Transduct Target Ther. 2024;9(1):38.
7. Drzewoski J, Kasznicki J, Trojanowski Z. The role of metabolic memory in the natural history of diabetes mellitus. Pol Arch Med Wewn. 2009;119(7–8):493–500.
8. Lachin JM, Nathan DM. Understanding metabolic memory: the prolonged influence of glycemia during the diabetes control and complications trial (DCCT) on future risks of complications during the study of the epidemiology of diabetes interventions and complications (EDIC). Diabetes Care. 2021;44(10):2216–24.
9. Miller RG, Orchard TJ. Understanding metabolic memory: a tale of two studies. Diabetes. 2020;69(3):291–9.
10. Conte C, Terruzzi I, Ambrosio G. Metabolic memory in diabetes: permanent scar, legacy, or ongoing domino effect? Cardiovasc Res. 2022;118(1):4–6.
11. Zhang D, Wu Y, Li Z, Chen H, Huang S, Jian C, et al. MiR-144-5p, an exosomal miRNA from bone marrow-derived macrophage in type 2 diabetes, impairs bone fracture healing via targeting Smad1. J Nanobiotechnol. 2021;19(1):226.
12. Zhang D, Xiao W, Liu C, Wang Z, Liu Y, Yu Y, et al. Exosomes derived from adipose stem cells enhance bone fracture healing via the activation of the Wnt3a/β-catenin signaling pathway in rats with type 2 diabetes mellitus. Int J Mol Sci. 2023;24(5):4852.
13. Hofbauer LC, Busse B, Eastell R, Ferrari S, Frost M, Müller R, et al. Bone fragility in diabetes: novel concepts and clinical implications. Lancet Diabetes Endocrinol. 2022;10(3):207–20.
14. Rohm TV, Meier DT, Olefsky JM, Donath MY. Inflammation in obesity, diabetes, and related disorders. Immunity. 2022;55(1):31–55.
15. Maduka CV, Schmitter-Sanchez AD, Makela AV, Ural E, Stivers KB, Pope H, et al. Immunometabolic cues recompose and reprogram the microenvironment around implanted biomaterials. Nat Biomed Eng. 2024;8(10):1308–21.
16. O'Neill LA, Kishton RJ, Rathmell J. A guide to immunometabolism for immunologists. Nat Rev Immunol. 2016;16(9):553–65.
17. Nedosugova LV, Markina YV, Bochkareva LA, Kuzina IA, Petunina NA, Yudina IY, et al. Inflammatory mechanisms of diabetes and its vascular complications. Biomedicines. 2022. https://doi.org/10.3390/biomedicines10051168.
18. Antar SA, Ashour NA, Sharaky M, Khattab M, Ashour NA, Zaid RT, et al. Diabetes mellitus: classification, mediators, and complications; a gate to identify potential targets for the development of new effective treatments. Biomed Pharmacother. 2023;168:115734.
19. Sinder BP, Pettit AR, McCauley LK. Macrophages: their emerging roles in bone. J Bone Miner Res. 2015;30(12):2140–9.
20. Fan S, Sun X, Su C, Xue Y, Song X, Deng R. Macrophages-bone marrow mesenchymal stem cells crosstalk in bone healing. Front Cell Dev Biol. 2023;11:1193765.
21. Huang Z, Iqbal Z, Zhao Z, Liu J, Alabsi AM, Shabbir M, et al. Cellular crosstalk in the bone marrow niche. J Transl Med. 2024;22(1):1096.
22. American Diabetes Association Professional Practice C. 2. Diagnosis and classification of diabetes: standards of care in Diabetes-2024. Diabetes Care. 2024;47(Suppl 1):S20–42.
23. Pantalone KM, Misra-Hebert AD, Hobbs TM, Wells BJ, Kong SX, Chagin K, et al. Effect of glycemic control on the diabetes complications severity index score and development of complications in people with newly diagnosed type 2 diabetes. J Diabetes. 2018;10(3):192–9.
24. Zhang D, Xiao W, Liu C, Wang Z, Liu Y, Yu Y et al. Exosomes derived from adipose stem cells enhance bone fracture healing via the activation of the Wnt3a/beta-Catenin signaling pathway in rats with type 2 diabetes mellitus. Int J Mol Sci. 2023;24(5).
25. Liu C, Liu K, Zhang D, Liu Y, Yu Y, Kang H, et al. Dual-layer microneedles with NO/O(2) releasing for diabetic wound healing via neurogenesis, angiogenesis, and immune modulation. Bioact Mater. 2025;46:213–28.
26. Tonna S, El-Osta A, Cooper ME, Tikellis C. Metabolic memory and diabetic nephropathy: potential role for epigenetic mechanisms. Nat Rev Nephrol. 2010;6(6):332–41.
27. Stehouwer CDA. Microvascular dysfunction and hyperglycemia: a vicious cycle with widespread consequences. Diabetes. 2018;67(9):1729–41.
28. Agarwal R, Filippatos G, Pitt B, Anker SD, Rossing P, Joseph A, et al. Cardiovascular and kidney outcomes with finerenone in patients with type 2 diabetes and chronic kidney disease: the FIDELITY pooled analysis. Eur Heart J. 2022;43(6):474–84.
29. Figeac F, Tencerova M, Ali D, Andersen TL, Appadoo DRC, Kerckhofs G, et al. Impaired bone fracture healing in type 2 diabetes is caused by defective functions of skeletal progenitor cells. Stem Cells. 2022;40(2):149–64.
30. Wang C, Ying J, Nie X, Zhou T, Xiao D, Swarnkar G, et al. Targeting angiogenesis for fracture nonunion treatment in inflammatory disease. Bone Res. 2021;9(1):29.
31. Sharifiaghdam M, Shaabani E, Faridi-Majidi R, De Smedt SC, Braeckmans K, Fraire JC. Macrophages as a therapeutic target to promote diabetic wound healing. Mol Ther. 2022;30(9):2891–908.
32. Shen Y, Zhang Y, Zhou Z, Wang J, Han D, Sun J, et al. Dysfunction of macrophages leads to diabetic bone regeneration deficiency. Front Immunol. 2022;13:990457.
33. Li M, Wei F, Yin X, Xiao L, Yang L, Su J, et al. Synergistic regulation of osteoimmune microenvironment by IL-4 and RGD to accelerate osteogenesis. Mater Sci Eng C Mater Biol Appl. 2020;109:110508.
34. Ye Q, Zhang M, Li Q, Jia L, Gao Y, Yuan H, et al. Regulation of the diabetic immune microenvironment by metformin-loaded strontium-doped mesoporous bioactive glass facilitates bone regeneration. J Mater Chem B. 2025;13(9):3114–27.
35. Liu ZY, Mao J, Li WQ, Xu CC, Lao A, Shin A, et al. Smart glucose-responsive hydrogel with ROS scavenging and homeostasis regulating properties for diabetic bone regeneration. Chem Eng J. 2024. https://doi.org/10.1016/j.cej.2024.154433.

36. Lim JC, Ko KI, Mattos M, Fang M, Zhang C, Feinberg D, et al. TNFα contributes to diabetes impaired angiogenesis in fracture healing. Bone. 2017;99:26–38.
37. Ruffell D, Mourkioti F, Gambardella A, Kirstetter P, Lopez RG, Rosenthal N, et al. A CREB-C/EBPbeta cascade induces M2 macrophage-specific gene expression and promotes muscle injury repair. Proc Natl Acad Sci U S A. 2009;106(41):17475–80.
38. Ren Q, Liu Z, Wu L, Yin G, Xie X, Kong W, et al. C/EBPβ: the structure, regulation, and its roles in inflammation-related diseases. Biomed Pharmacother. 2023;169:115938.
39. Zhu Y, Liu Y, Ma Y, Chen L, Huang H, Huang S, et al. Macrophage autophagy deficiency-induced CEBPB accumulation alleviates atopic dermatitis via impairing M2 polarization. Cell Rep. 2023;42(11):113430.
40. Yan L, Wang J, Cai X, Liou YC, Shen HM, Hao J, et al. Macrophage plasticity: signaling pathways, tissue repair, and regeneration. MedComm. 2020;5(8):e658.
41. Sun D, Chang Q, Lu F. Immunomodulation in diabetic wounds healing: the intersection of macrophage reprogramming and immunotherapeutic hydrogels. J Tissue Eng. 2024;15:20417314241265202.
42. Sen S, Xavier J, Kumar N, Ahmad MZ, Ranjan OP. Exosomes as natural nanocarrier-based drug delivery system: recent insights and future perspectives. 3 Biotech. 2023;13(3):101.
43. Li N, Hu L, Li J, Ye Y, Bao Z, Xu Z, et al. The immunomodulatory effect of exosomes in diabetes: a novel and attractive therapeutic tool in diabetes therapy. Front Immunol. 2024;15:1357378.

Publisher's Note